

# COMPARISON BETWEEN MEXICAN HAT AND HAAR WAVELET DESCRIPTORS FOR SHAPE REPRESENTATION

Adnan Abou Nabout and Bernd Tibken

*Chair of Automatic Control, Faculty of Electrical, Information and Media Engineering  
University of Wuppertal, Wuppertal, Germany*

**Keywords:** Image Processing, Shape Representation, Wavelet Transformation, Wavelet Descriptors.

**Abstract:** The wavelet transformation is a well known method in several engineering fields. In image processing and pattern recognition the wavelet transformation is used for the recognition of object shapes by deriving so called wavelet descriptors. In this context the Mexican Hat as well as the Haar function were used as mother wavelets. To derive wavelet descriptors the methods use a periodical angle function derived from the contour polygon. The angle function describes an object shape by calculating the angle changes along the object contour beginning from a given starting point. Since object shapes are described by polygons, the angle function is step-shaped and therefore it includes discontinuity at the existing polygon corners. This causes big changes of the Haar wavelet descriptors if the positions of the polygon corners change due to small changes of the object shape. Such changes can be caused at least by digitalization or binarization errors. The Mexican Hat wavelet descriptors are more adapted and suffer however from small changes. In this paper we present the results of the comparison between both methods in their accurateness of describing object shapes.

## 1 INTRODUCTION

The automatic recognition of objects, their classification or representation is a very important task in the field of image processing and pattern recognition. In particular, the recognition of object shapes is a commonly needed process in many applications in this area (Grenander, Chow and Keeman, 1991), (Belongie, Malik and Puzicha, 2001), (Fergus, Perona and Zisserman, 2003). The recognition of weed species classes in agricultural applications is one of the interesting examples for the importance of object recognition using shape information, since the shapes of weed species change according to the growing stages of the weeds (Nabou, Nour Eldin, Gerhards, Su and Kühbauch, 1994).

The most known method for the above mentioned task uses the Fourier analysis (Zahn and Roskies, 1972). The method is used to obtain a number of coefficients, called Fourier descriptors (FD) to describe a given object shape. The recognition can be done through the comparison between the FD of the unknown object with those of the stored object samples using minimum distance or

Fuzzy methods (Nabou, 1993). In (Nabou and Tibken, 2004, 2005, 2007 and 2008) we established an alternative method using Wavelet transformation. Similar to the FD we applied Wavelet descriptors WD using the Mexican Hat or Haar function as mother Wavelet.

In this paper we conclude the derivation of wavelet descriptors for both cases and compare the results of these different implementations in order to find out the appropriate Wavelet building set. To represent a given object shape we will show the right way how to apply a periodical angle function using the polygon data of a given object shape. This angle function must be free from any singularity which might arise due to object rotations. For that reason the paper shows the derivation of the angle function for a simple geometric object. To obtain a suitable number of WD we normalized the angle function over the interval  $[0 - 2\pi]$  and derived a wavelet building set in the same interval. The results are shown on the basis of different characters to illustrate the different steps. We also present some results related to the recognition of weed species in plant fields. The paper is organized as follows:

Section 2 addresses the derivation of the angle function and describes the problem of singularity. Section 3 introduces the continuous Wavelet transformation. The derivation of the WD using Mexican Hat as well as Haar function is presented in section 4. In section 5 the results of applying the new method are demonstrated and discussed. In this context the minimum distance approach is described, which is used to compare two different WD sets. In section 6 the starting point problem is discussed.

## 2 SHAPE DESCRIPTION USING AN ANGLE FUNCTION

To derive an angle function we use the polygon information of a given object shape derived after contour extraction and approximation (Nabou, 1993). Fig. 1 shows the example of a triangle shaped object (a) and his derived angle (red) and periodical angle functions (green) (b).

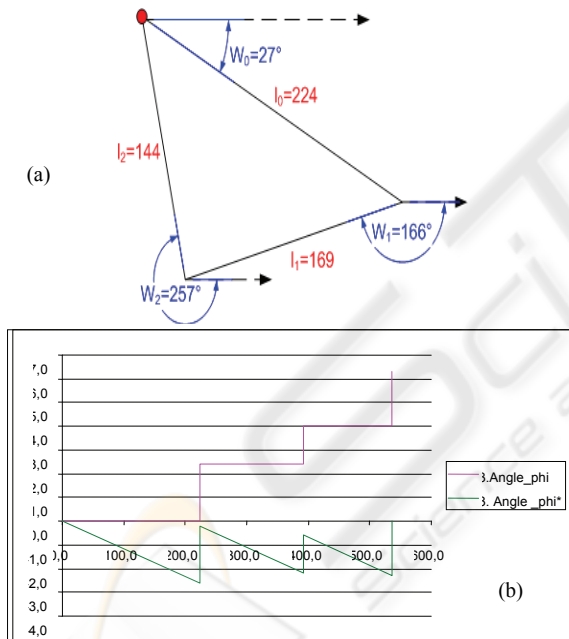


Figure 1: Polygon of triangle shaped object (a) and the angle functions of the given shape (b).

To obtain the angle function we calculate the angle differences between the absolute angles at every position on the given polygon and the absolute angle of the polygon at the starting point. It should be noted that the starting point depends on the object's position and orientation in the image. The calculation of the angle differences must take into account that the absolute angles can change

according to the object rotation. In some cases small object rotations cause significant changes in absolute angles. We denote this problem as singularity problem (Nabou, Tibken, 2008).

To avoid any singularity, we calculate all absolute angles of the polygon edges with respect to the x-coordinate as given in Fig. 1. The absolute angles of a polygon edge  $\overline{P_i P_{i+1}}$  are always positive and can be computed using the polygon data as follows:

$$\begin{aligned} & \text{if}(x_{i+1} \neq x_i) \\ & \quad \text{if}(y_{i+1} \neq y_i) \\ & \quad \left\{ \begin{aligned} & \omega = \tan^{-1}[(y_{i+1} - y_i)/(x_{i+1} - x_i)] \\ & \text{if}(x_{i+1} < x_i) \omega = \omega + \pi \\ & \text{else if}(y_{i+1} < y_i) \omega = \omega + 2\pi \end{aligned} \right. \\ & \quad \text{else if}(x_{i+1} > x_i) \omega = 0, \text{else } \omega = \pi \\ & \text{else if}(y_{i+1} > y_i) \omega = \pi/2, \text{else } \omega = 3\pi/2 \end{aligned}$$

where  $(x_i, y_i)$  and  $(x_{i+1}, y_{i+1})$  are the coordinates of the polygon corners  $P_i$  and  $P_{i+1}$ . To obtain the angle function we then calculate the angle differences as

$$\begin{aligned} \alpha_i &= \omega_i - \omega_0 \\ \text{if}(\alpha_i \geq \pi \ \& \ \alpha_i \leq 2\pi) \alpha_i &= 2\pi - \alpha_i \\ \text{else if}(\alpha_i \geq -2\pi \ \& \ \alpha_i \leq -\pi) \alpha_i &= -2\pi - \alpha_i \\ \text{else } \alpha_i &= -\alpha_i \end{aligned}$$

where  $\omega_i$  is the absolute angle of the polygon edge  $\overline{P_i P_{i+1}}$  and  $\omega_0$  the absolute angle of the first polygon edge  $\overline{P_0 P_1}$ . According to this definition, we obtain for the example in Fig. 1.a the angle differences  $(0^\circ, 139^\circ, 230^\circ)$ , which correspond to the radian values  $(0, 2.4, 4.0)$  as shown in Fig. 1.b.

The angle differences are negative in clockwise direction. The angle function  $f(l)$  (red colored function in Fig. 1.b) can be derived by calculating the value of  $\alpha$  for every position specified by the parameter  $l$ , where  $l$  is the contour length measured from the starting point up to the current contour position. The derived angle function is defined on the interval  $[0, L]$ , where  $L$  is the total length (circumference) of the given contour polygon and can be scaled on the  $[0, 2\pi]$ -interval using the following parameter transformation:

$$l \rightarrow t, \quad t = 2\pi l/L \quad (1)$$

with

$$f^*(t) = f(Lt/2\pi) - t \quad (2)$$

we receive a periodical angle function (green colored function in Fig. 1.b)  $f^*(t)$  with a period of  $2\pi$ .

### 3 WAVELET TRANSFORMATION

Similar to the FT, the WT uses elementary functions, called wavelets, to describe a given signal. In contrast to the FT, which uses harmonic functions with different frequencies, the WT uses only one basis wavelet (mother wavelet) to derive the reconstruction signals (Daubechies 1992). Through dilatation, compression and shifting of the mother wavelet, we derive new variants of this signal which together constitute the so-called wavelet building set. Equation (3) describes the general derivation of wavelets  $\Psi^{a,b}(t)$  from the mother wavelet  $\Psi(t)$  (Daubechies, 1992).

$$\Psi^{a,b}(t) = |a|^{-1/2} \Psi\left(\frac{t-b}{a}\right) \quad (3)$$

where  $a$  is the compression or dilatation parameter and  $b$  is the shifting parameter. Fig. 2 shows the mother wavelet based on the Haar function and some derived variants resulting from compression, dilatation and shifting using (3). Fig. 3 shows the equivalent Mexican Hat functions.

The function  $\Psi$  can be scaled over the interval  $[0, 2\pi]$  similar to the periodic angle function.

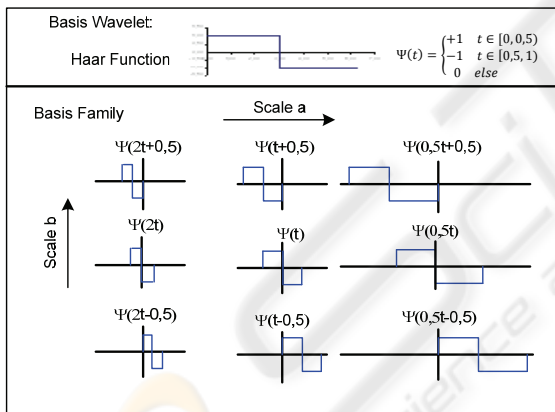


Figure 2: Wavelet building set based on Haar function.

Based on (3), the following equation shows the coefficient of the continuous Wavelet transformation  $W_{\Psi}f^*(a, b)$  for the derived angle function  $f^*(t)$  given in (2).

$$W_{\Psi}f^*(a, b) = |a|^{-1/2} \int_{-\infty}^{\infty} f^*(t) \Psi\left(\frac{t-b}{a}\right) dt \quad (4)$$

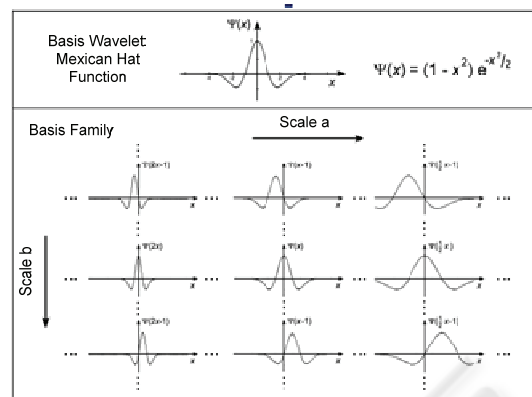


Figure 3: Wavelet building set based on Mexican Hat function.

Replacing the function  $\Psi$  in (4) by the scaled Haar function and setting the integration limits to  $[0, 2\pi]$ , we obtain the following expression:

$$W_H f^*(a, b) = |a|^{-1/2} \left[ \int_b^{b+a/2} f^*(t) dt - \int_{b+a}^{b+a/2} f^*(t) dt \right] \quad (5)$$

After executing the integrals in (5) we receive the following expression:

$$W_H f^*(a, b) = |a|^{-1/2} \left\{ b[f(l_j) - f(l_i)] - \sum_{m=i}^{j-1} \frac{2\pi}{L} l_m \alpha_m - (b+a)[f(l_k) - f(l_j)] + \sum_{m=j}^{k-1} \frac{2\pi}{L} l_m \alpha_m + \frac{a^2}{4} \right\} \quad (6)$$

where  $i, j, k$  are the indices of the polygon edges according to the position of the current used Haar function within the interval  $[0, 2\pi]$  and  $\alpha_m$  are the calculated angel differences (Nabout, Tibken, 2007).

Similar to (5) we receive (7) when we replace the function  $\Psi$  in (4) by the scaled Mexican Hat function.

$$\begin{aligned}
 W_M f^*(a, b) = & a\sqrt{|a|}(e^{-z_n^2} - e^{-z_0^2}) \\
 & - \sqrt{2|a|} b(z_n e^{-z_n^2} \\
 & - z_0 e^{-z_0^2}) \\
 & + 2a\sqrt{|a|}(z_n^2 e^{-z_n^2} \\
 & - z_0^2 e^{-z_0^2}) \\
 & - \sqrt{2|a|} \sum_{m=1}^n z_m e^{-z_m^2} \alpha_m \\
 & - 2\sqrt{2|a|} \pi z_n e^{-z_n^2}
 \end{aligned} \quad (7)$$

where

$$z_0 = \frac{1}{\sqrt{2}} \frac{b}{a}, \quad z_m = \frac{1}{\sqrt{2}} \left( \frac{2\pi l_m - bL}{aL} \right), \quad z_n = \frac{1}{\sqrt{2}} \left( \frac{2\pi - b}{a} \right).$$

In (6) and (7) the terms which include the angle differences  $\alpha_m$  are adequate to describe a given object shape.

We denote  $W_H f^*(a, b)$  as Haar Wavelet descriptor (H-WD) and  $W_M f(a, b)$  as Mexican Hat Wavelet descriptor (MH-WD).

#### 4 DERIVATION OF WAVELET DESCRIPTORS

To obtain suitable WD for representing a given object shape we vary the values of the compression or dilatation parameter  $a$  and the shifting parameter  $b$  according to the following equations:

$$a = r \frac{2\pi}{m}; \quad b = k \frac{2\pi}{m} \quad (8)$$

with  $m = \log_2(n)$  and  $n$ : number of WD

$$r \in \{1, 2, \dots, m\}$$

$$k \in \{0, 1, \dots, m-1\}$$

If we vary the parameter  $m$  as given in (8) we obtain a sufficient Wavelet building within the interval  $[0, 2\pi]$ . For  $m \leq 6$  is  $(a \geq 1)$  and (8) will deliver only components of the approximation signal. This signal describes the object shape roughly. Detailed signal information that describes small object shape changes can be derived for  $m > 6$  or through additional use of the reciprocal values of  $a$  as given in (8). Generally only a few number of WD (e.g. 32) is needed in practical recognition applications to describe different object shapes. In this case the parameter  $m$  can be set to 4 if we use the reciprocal value of  $a$  to include components of the detail signal. For  $m = 4$ , Fig. 4 shows a part of the Haar wavelet building set for different parameter values.

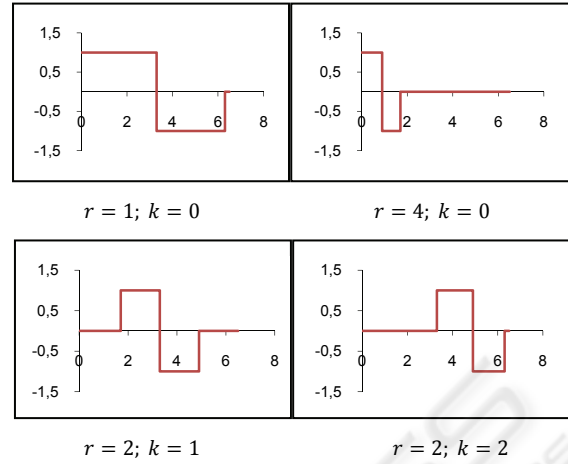


Figure 4: Part of the Haar wavelet building set derived within the interval  $[0, 2\pi]$ .

Fig. 5 shows the corresponding Mexican Hat wavelet building set for the same parameters.

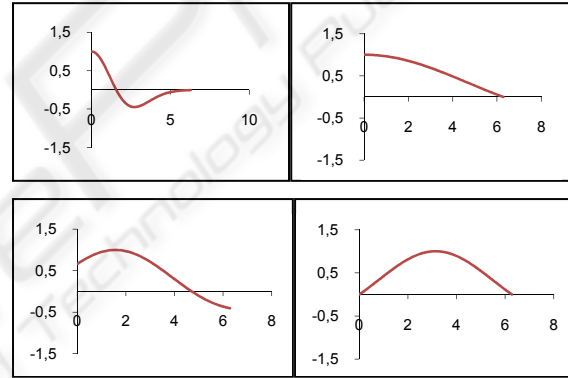


Figure 5: Part of the Mexican Hat wavelet building set derived within the interval  $[0, 2\pi]$ .

As shown in these figures small values of the parameter  $r$  produce compressed variants, big values on the other hand create dilated variants of the mother Wavelet. In both cases we receive an approximation signal of the Wavelet transformation, since  $a > 1$ . To receive components of the detail signal which describes small details of the contour shape we can use  $1/a$  in combination with the same values of  $b$ . For such values we obtain WD which are qualified to describe small matches between the compared shapes.

#### 5 RESULTS

Fig. 7 shows the 16 MH- as well as H-WD obtained from the approximation signal for the characters A and B as shown in Fig. 6. The used starting points of

the derived angle functions are marked in Fig. 6 in green colour. The dilatation or compress parameter  $a$  and shifting parameter  $b$  are calculated as given in (11) for  $r \in \{1, 2, 3, 4\}$  and  $k \in \{0, 1, 2, 3\}$ .



Figure 6: Example of an image with three characters.

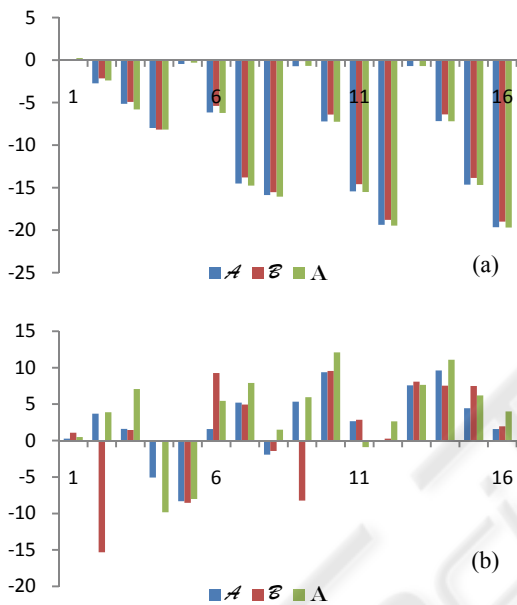


Figure 7: The first 16 MH (a) and H-WD (b) for the shapes of Fig. 6 obtained from the approximation signal.

As can be seen from Fig. 7 the differences between the MH-WD of the approximation signal are relatively small, the differences between the corresponding values of the H-WD are on the other hand large. This distinction is due to the discontinuity of the angle function, which causes big changes of the integration values in (6) when the Haar function jumps from negative to positive or positive to negative values. On the other hand the MH-WD indicate a periodical behaviour, so that only a few number of MH-WD of the approximation signal are needed to represent the given object shape. The H-WD on the other hand do not indicate such behaviour. This property carries forward even if we use different numbers of WD. Fig. 8 shows for instance the results of 25 WD of the approximation signal for  $r \in \{1, 2, 3, 4, 5\}$  and  $k \in \{0, 1, 2, 3, 4\}$ .

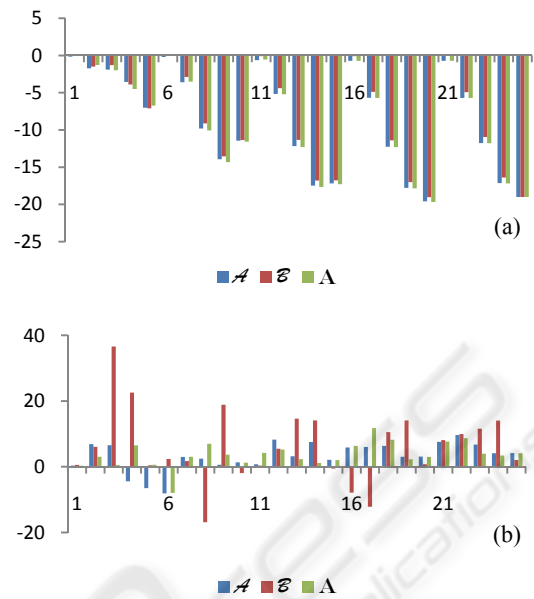


Figure 8: The first 25 MH and H-WD for the shapes of Fig. 6 derived from the approximation signal.

To study the detail signal we derived the 16 MH and H-WD obtained from the detail signal by using the same parameter  $b$  and the reciprocal value of the parameter  $a$  given before (Fig. 9).

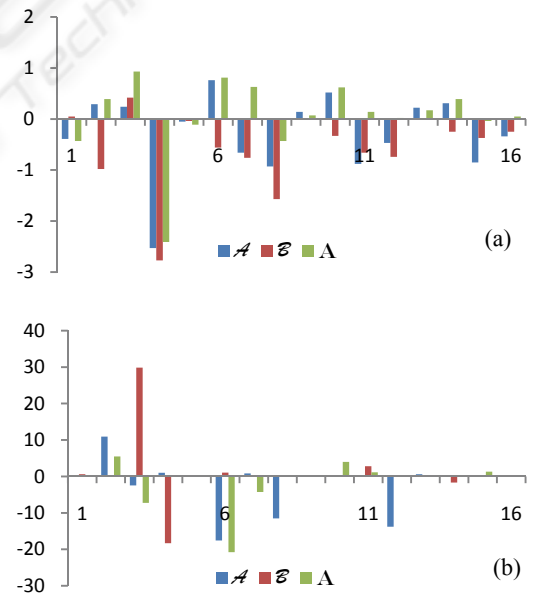


Figure 9: The first 16 MH and H-WD for the shapes of Fig. 6 derived from the detail signal.

The results in Fig. 9 indicate that the MH-WD of the detail signal do not show any periodical behaviour similar to the MH-WD of the

approximation signal. On the other hand the values of the detail signal are relatively small. In contrast to the values of the MH-WD, the H-WD of the detail signal show relatively large differences.

To compare the WD between different object shapes we use the Euclidean distances  $d$  as given in the following equation:

$$d = \sqrt{\sum_{i=1}^n (WD_i - WD'_i)^2} \quad (9)$$

where  $WD_i$  are the values of the Wavelet descriptors for the first object shape and  $WD'_i$  are the values for the second one.

The following table shows the distances between the object shapes given in our example derived from the approximation and detail signal separately.

Table 1: Euclidean Distances between the Object shapes of Fig. 6 obtained from MH-WD and H-WD.

Approximation signal (MH-WD)	( $d_A$ )
„A“ / „B“	2,48
„A“ / „A“	0,90
„A“ / „B“	2,74

Detail signal (MH-WD)	( $d_D$ )
„A“ / „B“	2,35
„A“ / „A“	2,13
„A“ / „B“	3,22

Approximation signal (H-WD)	( $d_A$ )
„A“ / „B“	25,42
„A“ / „A“	11,22
„A“ / „B“	27,86

Detail signal (H-WD)	( $d_D$ )
„A“ / „B“	47,05
„A“ / „A“	20,81
„A“ / „B“	47,51

As shown in table 1 the distances between the similar characters A and A are relatively small and for the different characters A and B as well as A and B on the other hand relatively large. Due to these results it is possible to recognize the different object shapes A and B using the minimum distance method. In our example the characters can be recognized using only the Euclidean distances of the approximation signal. In many other applications it is required to use also the detail signal to include

more detail information about the local changes of the compared contour shapes.

The following example shows the results of applying the new method for the recognition of weed species (Fig. 10).

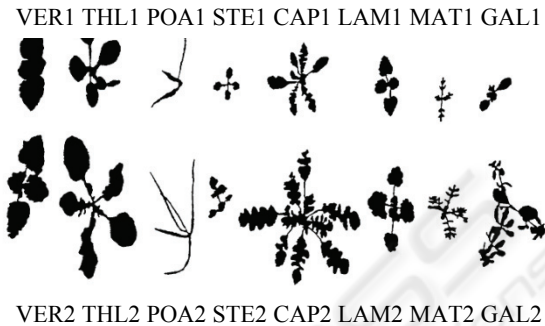


Figure 10: Eight weed species in different growth stages.

Table 2 shows the minimum distances between the WD of two different weeds using the WD components of the approximation and detail signal.

Table 2: Euclidean Distances between the weed LAM and MAT of Fig. 10 obtained from MH-WD and H-WD.

Approximation signal (MH-WD)	( $d_A$ )
„LAM1“ / „LAM2“	0,55
„LAM1“ / „MAT1“	1,18
„LAM2“ / „MAT1“	1,07

Detail signal (MH-WD)	( $d_D$ )
„LAM1“ / „LAM2“	1,77
„LAM1“ / „MAT1“	5,00
„LAM2“ / „MAT1“	5,52

Approximation signal (H-WD)	( $d_A$ )
„LAM1“ / „LAM2“	61,50
„LAM1“ / „MAT1“	94,32
„LAM2“ / „MAT1“	72,92

Detail signal (H-WD)	( $d_D$ )
„LAM1“ / „LAM2“	73,50
„LAM1“ / „MAT1“	114,85
„LAM2“ / „MAT1“	128,08

As shown in table 2 the weed can be recognized correctly using the minimum distance method even when we use either the approximation or the detail signal alone. For some other weeds (VER and LAM) the recognition process has failed.

## 6 THE STARTING POINT PROBLEM

The results of table 1 are obtained according to the chosen starting points (green colored positions in Fig. 6). If the starting points change, the angle functions will also be changed and with them the corresponding WD. If we change the starting point of the character  $\mathcal{A}$  for instance from the green colored position to the red one we receive for this character the following MH-WD and H-WD values (Fig. 11). Here both approximation and detail signals are drawn in the same diagram.

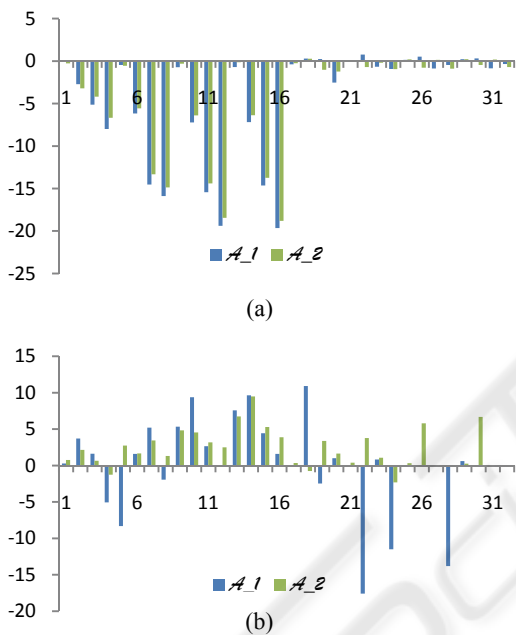


Figure 11: The MH-WD (a) and H-WD (b) for the character  $\mathcal{A}$  for the two different starting points given in Fig. 6 derived from the approximation and detail signal.

As shown in Fig. 11 the change of the starting point leads to large changes of the WD. Since the position of the starting point in real applications depends on several parameters, which cannot be fixed, like position and rotation of the objects in the image, number of objects, extraction method etc., the recognition process using the minimum distance method will fail. Table 3 reports the Euclidean distances between the given characters A and B derived from the MH-WD for the new starting point of the character A (red position). Using the H-WD instead of the MH-WD indicates similar behavior.

Table 3: Euclidean Distances between the Objects of Fig. 6 derived from the MH-WD for the red starting point.

Approximation signal	( $d_A$ )
$\mathcal{A}^c / \mathcal{B}^c$	4,43
$\mathcal{A}^c / \mathcal{A}^c$	6,86
$\mathcal{A}^c / \mathcal{B}^c$	2,74

Detail signal	( $d_D$ )
$\mathcal{A}^c / \mathcal{B}^c$	2,73
$\mathcal{A}^c / \mathcal{A}^c$	2,64
$\mathcal{A}^c / \mathcal{B}^c$	3,22

As shown above the distances between the characters with the similar shapes A and A are higher than the distances between the different shapes A and B as well as A and B. This is due to the change of the angle functions within the interval  $[0 - 2\pi]$  according to the change of the starting points. The following figure (Fig. 12) shows the angle functions of the character A for the two different starting points.

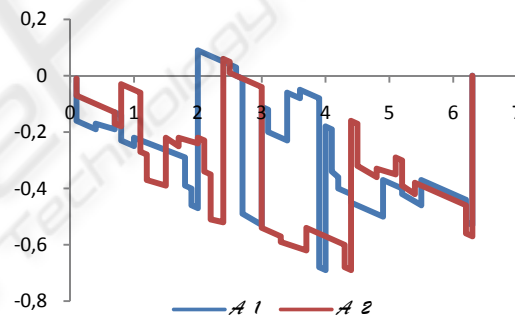


Figure 12: The angle functions of the characters  $\mathcal{A}$  for two different starting points.

As expected, the figure shows big differences of the angle functions related to the change of the starting point. Since the starting point on the contour depends on several parameters of the image, the above mentioned issue can cause confusion in recognition tasks, because it is not explicit clear whether big values of the Euclidean distance are related to shape differences or to different starting points. To solve this problem we use the following strategy:

Suppose we have a number of object samples  $O_j$  and an unknown object O which must be classified to one of the given object classes. The procedure can then be done as follows:

- Calculate the WD of all objects  $O_j$  for an arbitrary starting point and store them in a data base.
- Calculate the WD sets for all possible starting points of the unknown object  $O$ . This can be done easily if we use the polygon description of the object contour and change the starting point from one polygon corner to the next.
- Compare the WD sets of the unknown object separately with the stored WD of the object samples using the minimum distance method. We receive a number of Euclidean distances  $d_{ij}$ ;  $i = 1, 2, \dots, n$ ;  $j = 1, 2, \dots, m$  according to the number of different starting points  $n$  used in step 2 and the number of object samples  $m$  given in step 1.
- Find the minimum value of  $d_{ij}$ . The stored object sample related to this minimum value  $j$  represents the recognized object.

## 7 CONCLUSIONS

The representation of object contours using wavelet descriptors is useful in object recognition tasks. In particular, the Mexican Hat as well as Haar function are qualified to be used as a mother wavelet to obtain a sufficient number of WD which can be used in recognition tasks. The WD can be calculated very easily using (6) for the H-WD and (7) for MH-WD. The number of WD needed to recognize a given object increases according to the complexity of the object shapes and must be set according to the given application. It is possible in some cases to use only the components of the approximation signal in order to recognize an unknown object using the minimum distance method, but generally the use of the detail signal will include detail information about small differences between the compared object shapes. The starting point on the contour has a big influence on the recognition process, since the values of the WD depend strongly on it. The paper describes one possible solution where not only one set of WD is computed and compared with the stored WD of the object samples, but several sets of WD according to the different starting points.

## REFERENCES

- Grenander, U., Chow, Y. and Keenan, D. M., 1991. HANDS: A Pattern Theoretic Study Of Biological Shapes. Springer Verlag.
- Belongie, S., Malik, J. and Puzicha, J., 2001. Matching shapes, In ICCV, pp. 1.454-461.
- Fergus, R., Perona, P. and Zisserman, A., 2003. Object class recognition by unsupervised scale-invariant learning. In CVPR, pp. 264-271.
- Nabout, A., Nour Eldin, H.A., Gerhards, R., Su, B., Kühbauch, W., 1994. Plant Species Identification using Fuzzy Set Theory, pp. 48-53, Proc. of the IEEE Southwest Symposium on Image Analysis and Interpretation, Dallas, Texas, USA.
- Zahn, C., Roskies, R. Z., 1972. Fourier descriptors for plant closed curve, IEEE Trans. On C-21.
- Nabout, A., 1993. Modular Concept and Method for Knowledge Based Recognition of Complex Objects in CAQ Applications, VDI Publisher, Series 20, No. 92.
- Nabout, A., Tibken, B., 2004. Object Recognition Using Polygons and Wavelet Descriptors, 1st International Conference on Information & Communication Technologies, Proceedings of ICTTA'04, April 19 - 23, Damascus, Syria.
- Nabout, A., Tibken, B., 2005. Wavelet Descriptors for Object Recognition Using Mexican Hat Function, 16th IFAC World Congress, Prague, Czech Republic.
- Nabout, A., Tibken, B., 2007. Object Shape Recognition using Mexican Hat Wavelet Descriptors, 2007 IEEE International Conference on Control and Automation, Guangzhou, CHINA - May 30 to June 1, pp. 1313-1318.
- Nabout, A., Tibken, B., 2008. Object Shape Description Using Haar-Wavelet Functions, the 3rd IEEE International Conference on Information & Communication Technologies: from Theory to Application, ICTTA'08, 7-11 April 2008, Umayyad Palace, Damascus, Syria.
- Daubechies, I., 1992. Ten Lectures on Wavelets, Society for Industrial & Applied Mathematics.